

Channel Modeling for Wireless Body Area Networks

David B. Smith and Leif W. Hanlen

Abstract Wireless body area networks (BANs) are the latest generation of personal area networks (PANs) and describe radio networks of sensors, and/or actuators, placed in, on, around and some-times near the human body. BANs are motivated by the health-care application domain where reliable, long-term, operation is paramount. Hence understanding, and modeling, the body-area radio propagation channel is vital. In this chapter we describe channel models for wireless body area networks, in terms of operating scenarios—including on the human body, off the body, in the body, and body-to-body (or interfering); carrier frequencies from hundreds of MHz to several GHz; and bandwidth of operation, including narrowband and ultra-wideband. We describe particular challenges for accurate channel modeling such as the absence of wide-sense-stationarity in typical on-body narrowband BANs. We describe results following from a large amount of empirical data, and demonstrate that the BAN channel is dominated by shadowing with slowly-changing dynamics. Finally two particularly challenging scenarios for BAN operation are described: sleep-monitoring and also where there is a large number of co-located BANs.

Keywords Channel modeling • Radio propagation • Wireless body area networks

D.B. Smith (✉)

NICTA, 7 London Circuit, Canberra, ACT 2601, Australia

Australian National University (ANU), Canberra, ACT 0200, Australia

e-mail: David.Smith@nicta.com.au

L.W. Hanlen

NICTA, 7 London Circuit, Canberra, ACT 2601, Australia

Australian National University (ANU), Canberra, ACT 0200, Australia

University of Canberra, University Drive, Bruce, ACT 2617, Australia

e-mail: Leif.Hanlen@nicta.com.au

1 Introduction

Wireless body area networks (BANs) are radio networks of sensors and/or actuators, placed on, in, around and/or near the human body, and represent the latest generation of personal area networks. As such, BANs describe radio networks that will often employ ultra-low-power short-range radios. One of the principal application domains of BANs is for use in health-care, with other applications including consumer fitness, emergency services and consumer entertainment. Considering application in health-care, long-term, reliable operation at low-power is very important. We will show that reliable operation is a real challenge for BANs by considering typical characteristics of the radio channel. It is also then very important, so that system design can respond to these characteristics, to derive appropriate channel models for the BAN radio channel.

The main focus of this chapter will be the on-body radio channel, for communications from one location on a given subject's body to another location on the subjects body, which is envisaged as the most common BAN implementation. However there will be some focus on the off-body channel and the body-to-body channel. The body-to-body channel is important due to the anticipated prevalence of body area networks, where this interfering channel, with multiple co-located BANs, can dominate the on-body radio channel. It will be shown that there are various difficulties in channel modeling for BAN, which are particular to the BAN channel, underlining the importance of BAN reliability and life-time enhancing system design, such as relay-assisted communications, transmit power control and link adaptation. Important first and second-order statistics can be derived from extensive empirical campaigns, and alternate evaluations can be given directly from empirical data. The "everyday" BAN channel scenario presents a challenging environment for radio propagation and system design, but there are even more challenging environments in which BANs can operate, namely monitoring a person sleeping, and where there is a large number of coexisting BANs, which we will address.

2 Operational Scenarios for Wireless Body Area Network Channels

There are four scenarios for wireless body area network channels, namely

1. **On-body:** for radio communications from one part on the surface of the human body to another part on the surface of the human body;
2. **In-body:** for radio communications from inside the human body, typically to the body surface;
3. **Off-body:** for radio communications from the surface of the human body to a device closely located to the body, typically within 3 m of the body (or vice-versa, i.e., from off the body to on the body);

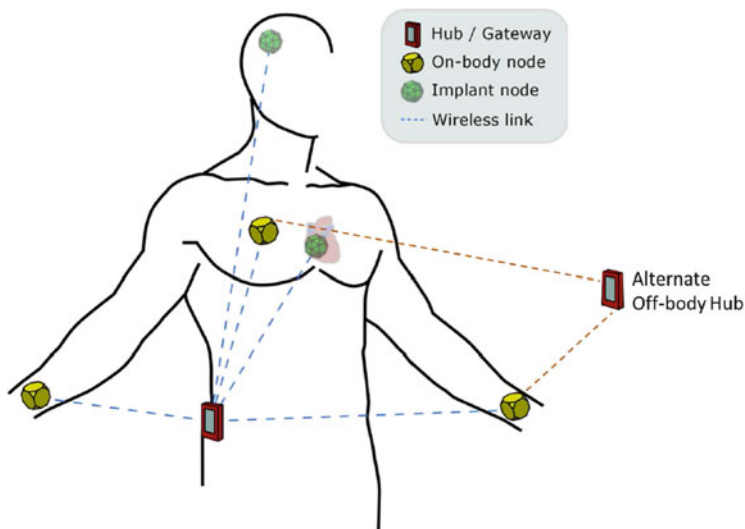


Fig. 1 BAN on a male subject, illustrating gateway (hub), sensors and in-body, on-body and off-body links, adapted from [44]

4. **Body-to-body or interfering:** for radio communications, target or interfering, from one subject's body to another subject's body.

A BAN on a subject, illustrating a gateway (hub), sensor nodes, on,-body in-body and off-body links, is shown in Fig. 1. The hub locations will be typically near the torso, either at the hips or on the chest; places where a subject could comfortably wear a device that is expected to be larger than a sensor node. These locations are also reasonably central on the human body.

We now describe the four scenarios in more detail, particularly with respect to challenges, operating environments and applications for each.

2.1 On-Body Channel

The on-body channel is the most prevalent channel for wireless body area networks and is the focus in this chapter. This channel will operate in various environments and will be dominated by slowly-varying dynamics from human-body movement and variations in shadowing by body parts. It presents significant difficulties to the radio systems designer, but there are also some benefits as follows:

- **Difficulties:** When operating with small low-power radios, long sensor/actuator radio lifetime is desired, thus requiring small power demands on the battery of the radio, as well as desired low electromagnetic radiation specific absorption rate (SAR) to the subject's body. This all leads to a desired transmit power

significantly less than 0 dBm (or 1 mW) , -10 dBm (or 0.1 mW) may often be desirable. Further, as will be described later, at typical carrier frequencies of several hundreds of MHz up to a few gigahertz, communication on the human body provides a difficult radio channel, where instantaneous path losses can become very significant and typical (or median) path losses for a lot of on-body radio links are still (relatively) very large. Further the variations in signal strength are not uniform, from one time interval to the next, such that the channel is in general not wide-sense-stationarity.

- **Benefits:** However there are a few benefits/aids available to the radio system designer from the typical on-body radio channel, particularly with narrowband communications in everyday environments:
 1. The channel shows reciprocity, that is the radio channel for communications from position a. to position b. on the body, has the same channel profile as for communications b. to a.;
 2. The channel, for the majority of on-body BAN usage, is stable for at least hundreds of milliseconds (typically more than 0.5 s), enabling relatively accurate channel prediction across multiple communications frames, simply with the last channel gain sample, which can help transmit power control and resource allocation;
 3. Although the direct, sensor-to-hub, link may be in outage, the slowly varying on-body channel, and possible postures of the human body, means there will often be another dual-hop link between source and hub, through suitably located relay/s transmission paths, giving significant reliability benefit to radio communications;
 4. Although the overall information transfer over the whole on-body BAN may be large, for typical applications such as in health-care, high data rates for particular links may not be required (often in orders of tens of kilobits per second);
 5. Finally for narrowband BAN communications, although the on-body channel is slowly time-selective, it is frequency non-selective, with no resolvable multipath, and one channel tap, such that inter-symbol interference (ISI) does not need to be mitigated.¹

2.2 *In-Body Channel*

The in-body channel will be, almost always, applied for medical applications, and mostly operate at lower carrier frequencies than the on-body channel. The main frequency of operation is most likely to be the medical implant communication system (MICS) band, which operates from 402–405 MHz. The in-body channel will

¹However, we note that for typical IR-UWB, broadband, communications, IEEE 802.15.6 compliant, there are approximately ten resolvable channel taps.

also predominantly be from implants/devices, with miniature radios, to radios on the surface of, or just outside the body. Transmission from one radio in the body directly to a radio in another location inside the body will be highly uncommon. The in-body channel, apart from transmissions at tens of MHz, will suffer from significant attenuation for radiowaves propagating through the body, and will often depend on radio propagation from the nearest body surface to the implant radio device [32].

With respect to the mentioned challenging properties of the on-body channel, the in-body channel will be affected by similar challenges. However restrictions with respect to output Tx power, and reducing battery power consumption are even further magnified, as it is desirable for batteries inside the human body to have a lifetime of several years (frequent surgery is not desirable), as well as reducing radio-wave absorption inside the human body.

As the in-body communication channel includes various additional components (e.g., creeping waves) we shall not discuss this further in this chapter as it is significantly different to the other parts. We note that there is some good description of in-body communications in, e.g. [4, 32].

2.3 Off-Body Channel

The off-body channel is the radio channel the most similar to standard small cell and personal area networks radio communications. However transmission from one part of the human body to a gateway/hub radio at a small distance from the human body will also often be dominated by shadowing, similar as for the on-body channel. It is also slowly time selective and a one-tap channel—but it can reasonably be expected that it is more wide-sense-stationary than the on-body channel, and also median path losses will often be lower, even though often over a greater distance than on-body links. In applications such as health-care, suitable placement of the radio device/s off the body may be particularly important to maximize the typical channel gains from desired off-body transmission, or to enhance the on-body communications, where one or more relays is placed off the human body. Also the off-body channel may have less energy-constrained relays than the on-body radio channel. All the other benefits for radio systems design for the on-body channel also apply for the off-body channel, such as reciprocity—but the data rates may sometimes be larger than for the on-body channel.

2.4 Body-to-Body (or Interference) Channel

In most wireless body area networks, it is unlikely that one network will be spread over multiple human bodies, apart from obvious exceptions for uses such as in the military and emergency services. But the body-to-body radio channel characteristics

are still very important, as in many cases for BAN operation there will be some, or significant, mobility, which coupled with the large anticipated large take-up of BANs, implies there will often be multiple people wearing BANs closely located, requiring coexistence without coordination between BANs. Thus, understanding radio propagation from one BAN to the sensor, relay or hub, of another BAN becomes very important.

This interfering channel will often demonstrate lower path losses than for an on-body Tx/Rx radio link-of-interest, due to on-body shadowing, and a lack of shadowing from the body-to-body interfering channel. Further the body-to-body channel does not demonstrate free-space path loss, and is strictly not distance dependent, unless a slowly varying shadowing factor is added to a distance-based path loss description with a larger path loss exponent than free space. The dynamics of the on-body channel, and body-to-body channel, are also similar to each other in that they are slowly time selective and frequency non-selective when considering narrowband communications.

The operation of BANs can also be significantly enhanced, when co-located with other BANs experiencing body-to-body interference, by both transmit power control and relay-assisted communications. In fact these two techniques may be particularly important to achieve performance benchmarks for on-body BANs to coexist with other BANs.

3 Technical Requirements for IEEE 802.15.6 BANs

There are various technical requirements, or, more precisely, guidelines for BANs from the IEEE 802.15.6 [47]. These broadly represent how BANs should operate and significantly influence key parameters for channel modeling.

- BANs should be scalable up to 256 nodes.
- A BAN link should support bit-rates between 10 kb/s and 10 Mb/s.
- The packet error rate (PER) should be $\leq 10\%$ for a 256 octet payload (i.e., 256×8 bits of data) for the 95 % best-performing links according to PER (i.e., at a given signal-to-noise ratio, those 5 % of channels that give the worst PER performance should not be used to determine whether this PER guideline is met).
- Maximum radiated Tx power should be 0 dBm (or 1 mW), and all devices should be able to transmit at -10 dBm (or 0.1 mW).² This automatically meets specific-absorption-rate (SAR) guideline of the FCC of 1.6 W/kg in 1 g of body tissue [13] (which equates to a max Tx radiated power of 1.6 mW).
- Nodes should be able to be added and removed (insertion/de-insertion) to/from the network in less than 3 s.
- Reliability, latency (delay) and jitter (variation of one-way transmission delay) should be supported for those BAN applications that need them. Latency in

²Please note this maximum Tx power is a requirement in the standard.

medical applications should be less than 125 ms, and should be less than 250 ms in non-medical applications. Jitter should be less than 50 ms.

- Power saving mechanisms (such as duty cycling) should be provided.
- The physical layer should support co-located operation of at least ten randomly distributed BANs (i.e. up to 2,560 nodes) in a $6 \times 6 \times 6m^3$ volume.
- In-body BAN and on-body BAN should coexist in and around the body.

4 Narrowband and UWB Radio Channels for BANs

BANs can use narrowband communications or UWB communications, classifications in terms of carrier frequencies and bandwidths are given in Table 1. We exclude mm-wave communications, such as at 60 GHz carrier frequency, as there is no BAN specification for this, and with very large path losses around the body at these frequencies, reliable communications is very difficult. We also exclude optical wireless and human-body communications (using body conduction), as typical radios do not use these techniques.

4.1 BAN Propagation Scenarios

There are two physical layer radio propagation methods defined by the IEEE 802.15.6 BAN standard [23],

1. Narrowband communications: The use of narrowband in healthcare has been described extensively, e.g., [17, 24]. Narrowband communications is better suited to most healthcare applications due to its lower carrier frequencies that suffer less attenuation from the human body and due to better established electromagnetic compatibility. Its smaller bandwidth (1 MHz or less) also means that multipath is unlikely to cause significant inter-symbol-interference (ISI) [36].

Table 1 Frequency bands and channel bandwidths (BW) for the two BAN radio propagation methods: Narrowband, Ultra-wideband [23]

Narrowband communications				UWB communications	
Frequency band	Bandwidth	Frequency band (MHz)	Bandwidth	Frequency band (GHz)	Bandwidth (MHz)
402–405 MHz	300 kHz	420–450	300 kHz	3.2–4.7	499
863–870 MHz	400 kHz	902–928	500 kHz	6.2–10.2	499
950–956 MHz	400 kHz	2,360–2,400	1 MHz		
2,400–2,483.5 MHz	1 MHz				

For any of the methods, IEEE 802.15.6 compliant devices must operate in one of the associated bands

2. Ultra-wideband (UWB) communications: Frequency-modulated FM-UWB and impulse-radio IR-UWB are both supported by the standard, with IR-UWB being better suited to BAN, because for IR-UWB noncoherent receivers can be implemented very efficiently and promises low power consumption to meet stringent constraints on battery autonomy [26]. One particularly suitable application of UWB in BAN is in consumer electronics as UWB offers higher throughput due to its larger bandwidth; each UWB channel has a bandwidth of 499 MHz in IEEE 802.15.6 [23].

5 Suitable Small-Scale First Order Statistics of BAN Channels

First-order small-scale statistical modeling of narrowband channels, has been performed by fitting statistical distributions that are commonly used to describe fading (Rayleigh, normal, lognormal, Ricean, Nakagami-m, Weibull, gamma) to measured channel gain (channel gain is the inverse of path loss) data, e.g., [8, 17, 35, 39], and, some unusual (e.g., kappa-mu ($\kappa - \mu$)) distributions [9]. Statistical modeling of channel gain has mostly been performed indoors e.g., [17, 35]. A chart that summarizes the distributions considered, from [44], is given in Fig. 2.

In general, lognormal, gamma and Weibull are most-often found to be a best-fit.³ Whilst Nakagami-m is often attempted as a fit, it has a smaller success rate; and Ricean has considerably smaller success rate than Nakagami-m. Further, it is very clear from Fig. 2 that the Rayleigh distribution is a poor fit for almost every scenario and environment for which it is attempted. Conversely, for any distribution, an author has invariably found at least one scenario that fit.

The lognormal, gamma and Weibull distributions are specified as follows:

- Lognormal

$$f(x|\mu_l, \sigma_l) = \frac{1}{x\sigma_l\sqrt{2\pi}} \exp \left\{ -\frac{(\ln(x) - \mu_l)^2}{2\sigma_l^2} \right\}, \quad (1)$$

where $\ln(\cdot)$ is the natural logarithm.

- Gamma

$$f(x|a, b) = \frac{1}{b^a \Gamma(a)} x^{a-1} \exp \left\{ -\frac{x}{b} \right\}, \quad (2)$$

where $\Gamma(\cdot)$ is the Gamma function.

³According to the ratio of the first two bars for each of these in Fig. 2 (only considering those distributions tested ten or more times.)

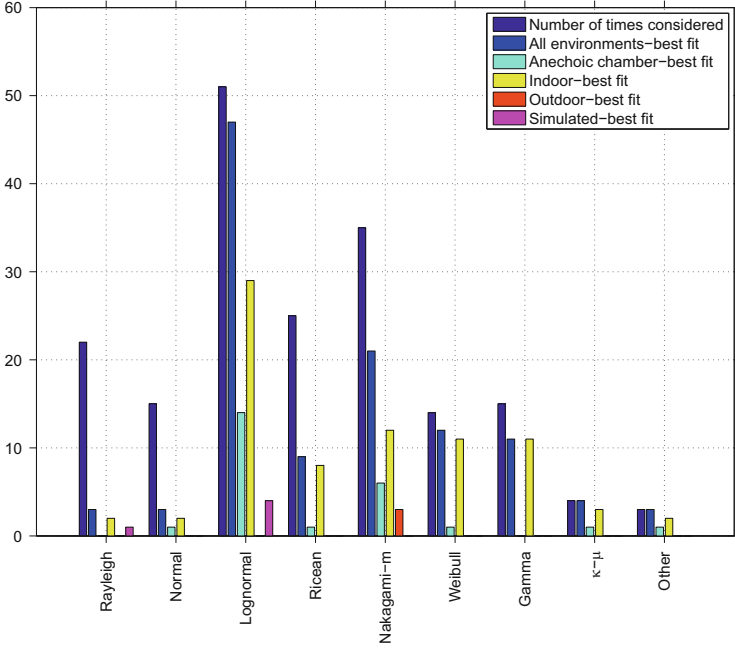


Fig. 2 Distributions, number of times considered, and times found to be best fit for all environments and per-environment from [44]. “Other” includes one log-logistic and one $\eta-\mu$ distribution, as well as one distribution representation by empirical histogram representations of channel gain data

- Weibull

$$f(x|a_w, b_w) = b_w a_w^{-b_w} x^{b_w-1} \exp \left\{ -(x/a_w)^{b_w} \right\}. \quad (3)$$

We now give three example narrowband scenarios where the lognormal, Weibull, and gamma distributions are good fits for measured fading statistics of channel gain data, all scenarios’ data is open-access [43].

5.1 Experimental Narrowband Measurement Campaigns

1. *On-Body*: We captured hundreds of hours of on-body channel gain data for “everyday” mixed activity of ten different adult subjects, using a range of transceiver Tx/Receiver(Rx) locations. The everyday mixed activity included indoor office work, at-home general activity, driving in a car and jogging outdoors, as well as transitions between each activity. Small wearable radios as described in [19], were used to capture the data. The radios transmit 540 kHz

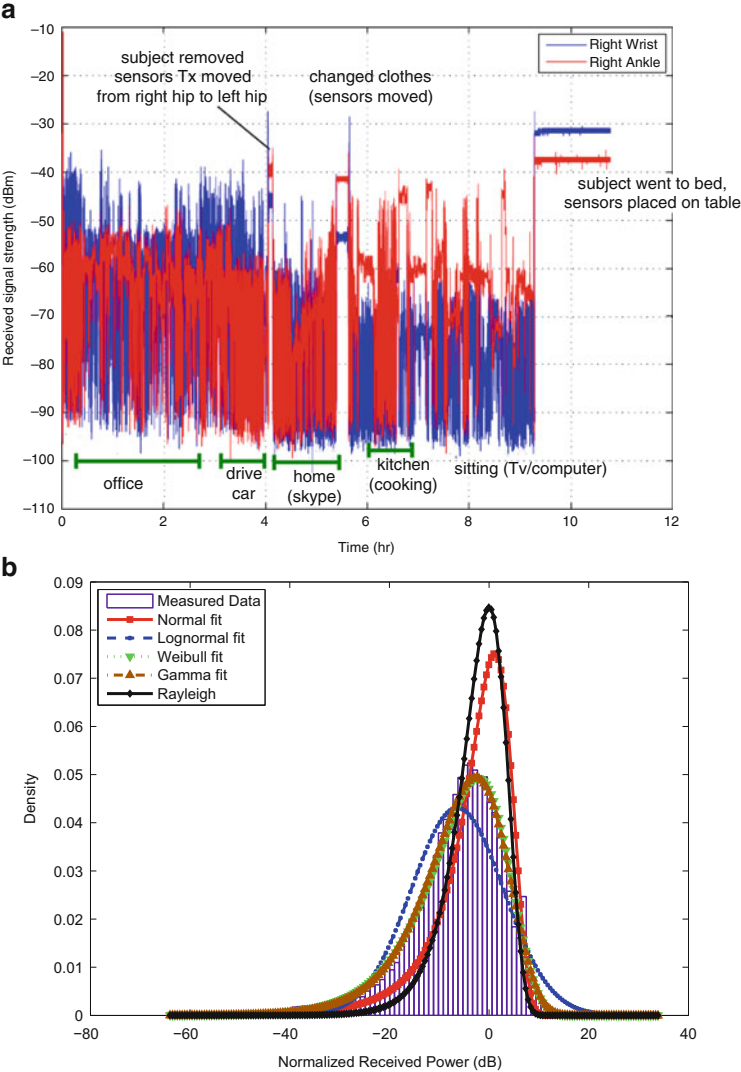


Fig. 4 Typical “everyday” channel gain profiles for one subject and agglomerate PDF over ten subjects. (a) Typical channel gain profile over 9 h for “everyday” activity from [41]. (b) PDF on-body channel gain agglomerate from everyday activity of ten subjects, 540 kHz bandwidth at 2,360 MHz [39]

Table 2 First-order statistics fits to everyday activity channel sounder channel-gain data, where the data has been normalized to mean of each link data-set [46]

Radio tx–Rx link	Mean channel gain (dB)	Median channel gain (dB)	Gamma distribution
Left hip–Chest	−50.1	−62.5	$a = 1.59, b = 0.486$
Left hip–Left wrist	−53.8	−61.7	$a = 1.44, b = 0.472$
Left hip–Right wrist	−60.2	−69.1	$a = 1.82, b = 0.431$
Left hip–Right ankle	−61	−69.7	$a = 2.16, b = 0.38$
Left hip–Head	−64.3	−71.2	$a = 2.17, b = 0.372$
Chest–Left wrist	−58.4	−62.5	$a = 1.82, b = 0.412$
Chest–Right wrist	−66.3	−70	$a = 1.86, b = 0.419$
Chest–Right ankle	−69.4	−77.5	$a = 2.63, b = 0.317$
Chest–Left ankle	−78.8	−82	$a = 2.9, b = 0.29$
Left hip–Right hip	−53.2	−83.5	$a = 2.31, b = 0.348$
Overall	−56.4	−69.8	$a = 1.81, b = 0.43$
O’ all no normalization	–	–	$\text{LN}(\mu_l = -7.74, \sigma_l = 1.1)$

The gamma distribution (2), is the best fitting distribution type for this data, apart from overall sets, non-normalized, which is lognormal (LN), (1)

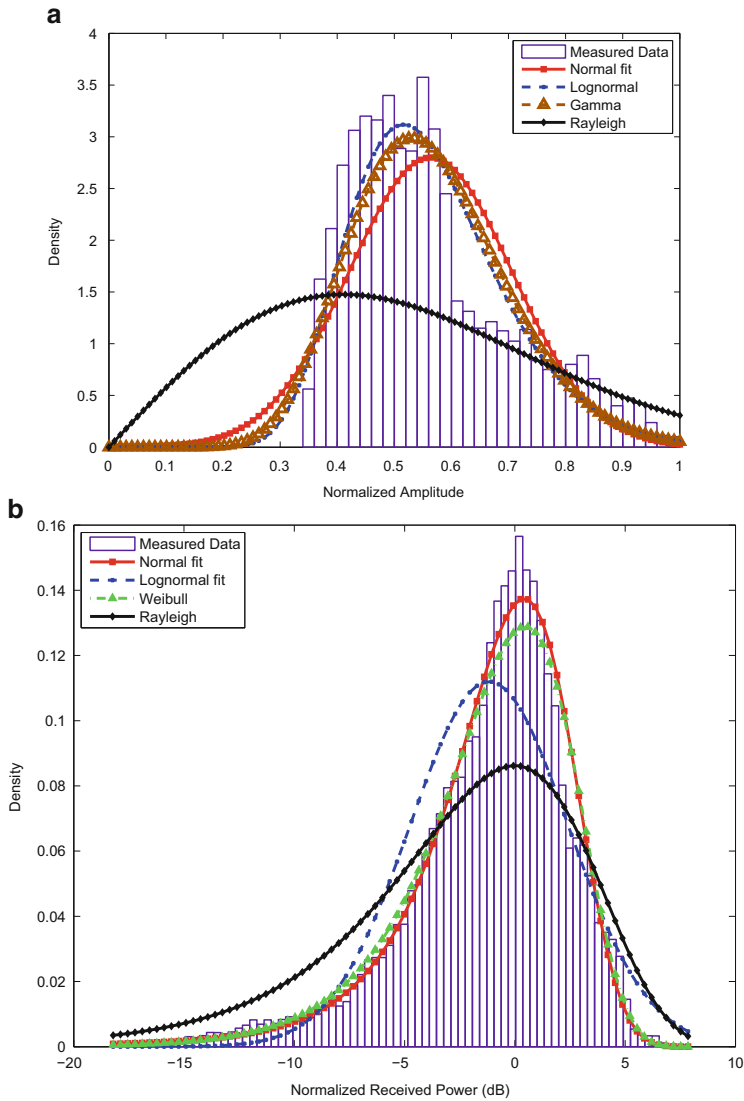


Fig. 5 On-body and off-body probability density functions (PDFs) with running and walking activity respectively from [39]. (a) PDF back to chest, running, 10 MHz bandwidth at 2,360 MHz. (b) PDF off-body agglomerate of subject walking, 10 MHz bandwidth, at 820 MHz

Table 3 Agglomerate scenarios, bandwidths and the best fitting model with parameters (in brackets) to those off-body scenarios at 427 MHz, 820 MHz and 2.36 GHz [39]

Action	Carrier frequency (MHz)	Bandwidth	Fading distribution
Moving	820	10 MHz	Weibull, ($a_w = 1.05, b_w = 3.04$)
Moving	2, 360	10 MHz	Nakagami-m, ($m = 1.6, \omega = 1$)
Moving	427	100 kHz	Weibull, ($a_w = 1.02, b_w = 2.25$)
Moving	2, 360	100 kHz	Weibull, ($a_w = 1.01, b_w = 2.15$)
Standing	820	10 MHz	Lognormal, ($\mu_l = -0.000839, \sigma_l = 0.0289$)
Standing	2, 360	10 MHz	Gamma, ($a = 384, b = 0.0026$)
Standing	427	100 kHz	Gamma, ($a = 44, b = 0.0224$)
Standing	2, 360	100 kHz	Normal, ($\mu = 0.987, \sigma = 0.161$)

for 5 s. Measurements were taken with a vector signal analyzer (VSA) with the test subject placed in four different locations in a room, with set-up in Fig. 3b. The horizontal distance between the test subject and Rx was either 1, 2, 3 or 4 m at each location. At each location measurements were taken with the subject facing in four directions: 0° , 90° , 180° and 270° , with 0° when the subject faced the Rx and 90° when he moved 90° clockwise from the 0° position. In Fig. 5b the best-fitting distribution to channel gain is Weibull for the scenario of the subject Walking, 10 MHz bandwidth, at 820 MHz carrier frequency, considering all distances and directions [39]. The lognormal distribution also provides a good fit in Fig. 5b. A summary table of best fitting distributions for all scenarios is given in Table 3.

5.2 First-Order UWB BAN Channel Modeling

The lognormal distribution is by far the most commonly found best fit for UWB BAN channels, this lognormal fit, and measurements campaigns used in this characterization, can be found in, e.g., [11, 15, 31]. BAN channels, particularly those with large bandwidths, contain a large number of factors that contribute to the attenuation of the transmitted signal; these include diffraction, reflection, energy absorption, antenna losses, etc. . . , which are additive in the log-domain [15]. The addition of multiple lognormally distributed paths results in another lognormal distribution.⁴ When compared to narrowband BAN, there is also more large-scale fading with UWB from larger path losses due to its higher carrier frequencies [46].

⁴The negative effects of multipath are more common in UWB as there is increased inter-symbol interference (ISI) with its higher sampling rates.

5.3 *Difficulty Choosing the Best Channel Model*

It is clear from the variety of models and modeling techniques the choice of a most-suitable or best BAN model is difficult. There is also a bigger issue that we will address in the following section, that of non wide-sense-stationarity.

In terms of choosing the best statistical model, particularly according to small-scale first-order statistics, an argument has been made for separate characterization of individual links (i.e., from a Tx at a particular position to an Rx at another position on the body) in various literature [11, 35]. In fact, the best-fitting statistical distributions have often been specified with their relevant parameter estimates, according to particular positions on the body. However, in some studies, a fit to normalized agglomerate data from many on-body links, where each link's channel gain data is normalized by the mean path loss, i.e., mean-removed, is made for the whole-body with fewer parameters [39, 41]. This is often preferable, because channel dynamics are more important than the static attenuation represented by the mean path loss for any individual link. Whilst a parameterized “model” might give better fit by specifying the precise location of the sensor nodes, such a model is useless to a sensor node designer: would they use different radios for each part of the body? Would a consumer be told: “this sensor only goes on your arm, this one only works on your ankle”? A good model fit in such a setup is meaningless.

5.4 *Body-to-Body Ban Interference Modeling*

The following summary of body-to-body BAN modeling, follows from description in [10], and further details can be found in [10]. In [22] the body-to-body radio channel was investigated for carrier frequencies of 2.45 and 5.8 GHz with two subjects. Channel gains followed a gamma distribution with mean and variance values following a power law in terms of distance between two BANs; almost independent of carrier frequency but dependent upon on-body antenna position and body orientation. Small-scale Ricean fading was found with the Ricean K-parameter depending mainly upon on-body antenna position rather than Tx-Rx separation, while large-scale gamma fading was found at a constant distance, with large-scale lognormal fading when the distance changed randomly.

Investigations on UWB body-to-body communications have been described in [33]. Measured data was obtained in an anechoic chamber for two subjects standing at various distances with different body orientations and showed that the path loss was strongly related to the placement of the devices on the body as well as to the relative position of the human bodies.

In [20] it was shown, for an indoors environment, that the interference channel gain is dominated mostly by subject movements and not the distance between BANs. The results showed that the signal-to-interference-ratio could be very low, with greater interfering channel gain, than for target on-body signal, because of significant shadowing from the human body. It was also shown that on-body links and interfering links are uncorrelated.

6 Important Second-Order Statistics for BANs

The BAN channel is significantly influenced by the movement of the wearer of the BAN (whether moving very slowly or quickly). Considering such BAN dynamics, second-order statistics are also important for characterizing BAN channels, both on-body and off-body. As also described in [44], the following summarizes key second-order statistical characterizations for BAN radio propagation:

1. Delay spread and the power delay profile of BAN channels can be used to determine the number of channel taps and hence the presence of inter-symbol interference (ISI). Significant multiple resolvable signal paths; i.e., significant multiple channel taps, and hence ISI, only occurs in the UWB BAN channel [16, 29]. This is different to the narrowband BAN channel, with bandwidths up to 10 MHz, which can be well-approximated by a single-tap channel [36]. This is an obvious result as the amount of ISI in a channel increases with its bandwidth. The 499 MHz UWB channel bandwidth specified for IEEE 802.15.6 [23] is approximately 50 times that of the peak narrowband channel bandwidth. Measurements using 500 MHz bandwidth IR-UWB report that more than 10 channel taps can be resolved [14].
2. Average fade duration—i.e., the average time the received signal strength is below any given level—can be used to determine the amount of time for which successful packet transmission on a given Tx/Rx link may not be possible. Hence it is an important parameter for BAN communications. The level crossing rate (LCR)—i.e., the average rate at which the signal strength crosses from above to below any given signal level (particularly at the mean path loss [38])—can be used to infer the rate of fading. The LCR can be used to determine the Doppler spread, which is approximately 1 Hz in “everyday” BAN channels [44], but can be above 4 Hz with someone running [37]. It has been determined that both average fade duration and level crossing rate are highly dependent on channel dynamics, as they depend on the rate and amount of body movement [38, 39]. In many typical BAN channels the average fade duration is 300 ms or more [38], significantly larger than the 250 ms latency requirement for many BAN applications [25] (as outlined in Sect. 3).
3. Autocorrelation of time-varying channel gain, which can be used to determine coherence time [37], for any BAN link can determine for how much time successful packet transmission is possible, as with average fade duration. Thus autocorrelation drives the design of packet lengths, as well as driving the placement of pilots for channel estimation, making it an important parameter for BAN communications. It is also important for power control based on channel prediction [40]. Longer coherence times, of up to 1 s for the ‘everyday’ mixed activity for on-body narrowband BAN channel [39, 40], allow for successful transmit power control over the duration of multiple BAN superframes (even when a superframe is hundreds of milliseconds in length). With continuous movement, the channel coherence time can drop to between 70 and 25 ms [37], indicating much smaller time for successful packet transmission.

4. Cross-correlation is of some importance and has been investigated in [11, 45]. It is important because BAN sensors may be densely placed on the body, and the quality of one gateway-to-sensor link could be used to determine the quality of the same gateway to another proximate sensor link via the cross-correlation of their signal strengths. However, we have found that with a medium density of 10 on-body sensors such spatial cross-correlation coefficients are 0.5 or lower.⁵ This may not be sufficient given that spatial cross-correlation is generally considered to be significant for values of 0.7 or greater.

7 Significant Issues in Wireless BAN Channel Modeling

There are several issues, or challenges presented, in determining suitable channel models for wireless BANs, which will be outlined here.

7.1 Statistical Fits: User Beware

The narrowband on-body BAN channel, is not wide-sense-stationary (WSS) outside timeframes of 500 ms or less [6], unlike networks such as mobile cellular communications and wireless LANs. This implies that any channel model, no matter how seemingly accurate, will provide a limited representation of the channel with respect to accuracy in terms of statistics of any order, across time, for all time.⁶ This implies that resource allocation, based on long-term statistical analysis, may not be a practical mechanism for narrowband BAN. Although lack of wide-sense stationarity has only been shown, thus far, for narrowband BAN, it can be reasonably be expected to also be present for UWB BAN. The fact that BAN radio channels are not wide-sense-stationary, calls into question the statistical fits in the open literature where WSS is implicitly assumed.

Amongst statistical fits, the Rayleigh distribution is a very poor choice for BAN fading statistics. Although the Rayleigh distribution is a good fit when various multipath in the radio channel are additive in the linear domain. Thus, in contrast to many other radio networks, the combinations of multipath that occur in the BAN are not additive in the linear domain—these effects are additive in the log-domain, as indicated by the good fit of the lognormal distribution; and the small-scale fading is also often dominated by shadowing, as indicated by the good-fit for gamma

⁵This is corroborated by results for 5 on-body sensors in [11].

⁶As wide-sense-stationarity is generally considered to be both necessary and sufficient for n th-order statistical channel characterization across time.

fading [1]. Although the Rayleigh model is a consistently poor fit in most cases, [12] notes “we can approximate the fading statistic with a Rayleigh distribution,” suggesting that a Rayleigh model might be useful in some cases.

Unfortunately, most authors provide only their goodness-of-fit result, based on their particular measurement and comparison criteria: one cannot retrospectively test if the measurements might support a new model choice, nor can one test the impact of an invalid stationarity assumption. This means that the models in the literature cannot necessarily be relied upon. The lack of reliable representation reinforces the need for large datasets, such as the “open-access” dataset [43], capturing many hundreds of hours of BAN link data, to test the appropriateness and validity of various radio system designs using deterministic modeling with respect to reliable empirical data, rather than statistical modeling. It also reinforces that traditional approaches to system design are not applicable to BANs and that the presumptions implicit in standard radio communications must be validated in BANs.

7.2 Issue: Path Loss for BAN Channels Is Not Well-Characterized by Propagation Distance

Some of the efforts for large-scale statistical modeling have been to model expected path loss in terms of distance for both narrowband and ultra-wideband propagation, and hence determine path loss exponents as a function of the carrier frequency, e.g., [4, 7, 15, 29]. A wide variation of path loss exponents for both narrowband and UWB, even within similar environments, have been reported, e.g., [3, 5, 15, 29]. Such variation suggests that the distance-based path loss modeling approach is poor; path loss exponents in the UWB bands for indoors measurements, have been reported from below 2 (better than free space) [29] to above 7 [15], and even up to 10 [3]. When measured in anechoic chambers, 2.4 GHz narrowband path loss exponents have been reported from below 3 [4], but have also been reported to be above 6 [48]. It is clear that path loss exponents are very much measurement campaign and environment dependent—this is more severe than simply “indoor” or “outdoor” and seems to indicate that the specifics of the building would be needed before distance-based path loss could be used reliably.

A distance-based path loss model, which ignores sensor placement and movement, produces a misleading model of the received signal strength for a BAN link. This is seen by measured path losses for set activities (standing, walking, and running) given in Table 4, see [28]. Two points are immediately clear:

1. the “distance” between the hip and wrist/ankle is very different for standing still vs running;
2. the path-loss is dominated by the whether-or-not of the path that includes the human body: the direct distance back-to-chest is much less than hip-to-ankle, yet the path loss is lower for the longer distance—because the path to the ankle is predominantly free-space, while back-to-chest is shadowed.

Table 4 Average path loss (dB), set activities, at 2.36 GHz [28].

Action	Receiver at right hip						Receiver at chest		
	Transmitter at						Transmitter at		
	Chest	Right wrist	Left wrist	Right ankle	Left ankle	Back	Right wrist	Right ankle	Back
Standing	65.3	44.5	74.7	60.9	70.7	75.3	70.5	66.3	73.0
Walking	59.1	47.3	59.8	53.9	58.5	67.4	64.9	62.4	72.0
Running	55.9	36.3	52.5	55.0	59.0	68.5	57.4	63.3	71.7

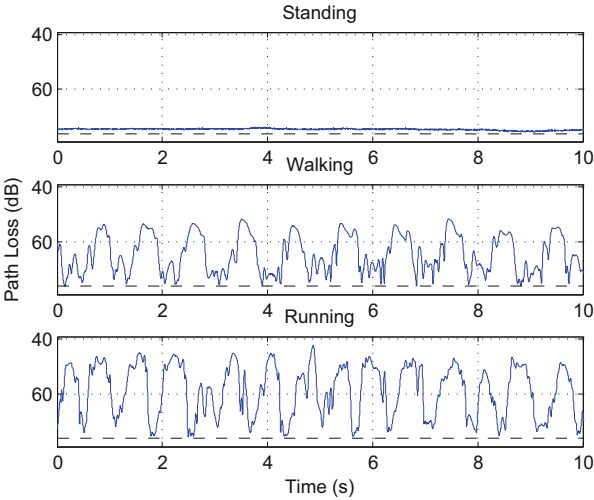


Fig. 6 Left wrist to right hip path loss v. time, 10 MHz bandwidth at 2.36 GHz [28], subject standing, walking and running

7.3 Issue: It Is Not Appropriate to Categorize On-Body BAN Links as Either Non-Line-of-Sight (NLOS) or Line-of-Sight (LOS)

Consider a left wrist to right hip link. Figure 6 shows a transition between NLOS and partially obstructed LOS as the subject movements increasing from standing to running. The subject is exposing and blocking the LOS link between the wrist and hip with their torso. Hence, characterizing a link as either LOS or NLOS is not meaningful for this link. The number of signal states is more than just LOS and NLOS, particularly with respect to dynamics, with moving body parts and changes in posture. It is more appropriate to capture the rate of movement and statistically characterize the path loss for this link.

8 Alternative Model Evaluations

Much of the previous statistical description has been based on relative comparisons of different statistical models. Here we provide an absolute measure, following from the description in [34, 41], to evaluate accuracy of channel models.

8.1 New Goodness-of-Fit Criterion to Characterize BAN Channel

In order to choose the best characterization of data we propose a goodness of fit function [34, 41]. This function, which represents a generalization of various criteria for model selection,⁷ for a model with p parameters $\boldsymbol{\theta} = \{\theta_1, \dots, \theta_p\}$ applied to data \mathbf{x} with n samples is:

$$\mathcal{G}\{\boldsymbol{\theta}, \mathbf{x}\} \triangleq \mathcal{E}\{\boldsymbol{\theta}, \mathbf{x}\} + \mathcal{C}\{\boldsymbol{\theta}, \mathbf{x}\}, \quad (4)$$

where $\mathcal{E}\{\cdot\}$ is an increasing function of error between model and data, and $\mathcal{C}\{\cdot\}$ is a monotonically increasing function of number of parameters, for a given number of samples. Here goodness-of-fit improves as $\mathcal{G}\{\cdot\} \rightarrow 0$.

The Akaike-information-criterion (AIC) [2] (which has previously been used to determine best BAN model selection, e.g., [15, 39]) can be represented according to the framework of (4),

$$\mathcal{G}_{\text{AIC}}\{\boldsymbol{\theta}, \mathbf{x}\} = \underbrace{\left[-2 \ln \left(L(\hat{\boldsymbol{\theta}} | \mathbf{x}) \right) \right]}_{\mathcal{E}_{\text{AIC}}\{\boldsymbol{\theta}, \mathbf{x}\}} + \underbrace{\left[2p + \frac{2p(p+1)}{(n-p-1)} \right]}_{\mathcal{C}_{\text{AIC}}\{\boldsymbol{\theta}, \mathbf{x}\}}, \quad (5)$$

where $\mathcal{G}\{\cdot\}$ implies goodness and $\ln(L(\hat{\boldsymbol{\theta}} | \mathbf{x}))$ is the maximized log-likelihood, based upon the maximum-likelihood estimate of model parameters $\boldsymbol{\theta}$, given the data \mathbf{x} .

For BANs with measurements across many Tx/Rx links the AIC approach suffers from the problem that it only provides an ordering of models. For different data sets with different parameterizations it is meaningless to compare AIC values. The goodness-of-fit form (4) can be used to develop a natural reference point, which is the joint empirical histograms of the many-link channel gain data sets. That is, given M data sets, we choose B histogram bins, and for each set $m = \{1, \dots, M\}$ find the histogram $H_m(b)$ with $b = \{1, \dots, B\}$. This ‘model’ has $P = M \times B$ free parameters.

⁷Hence this function is not limited to propagation data.

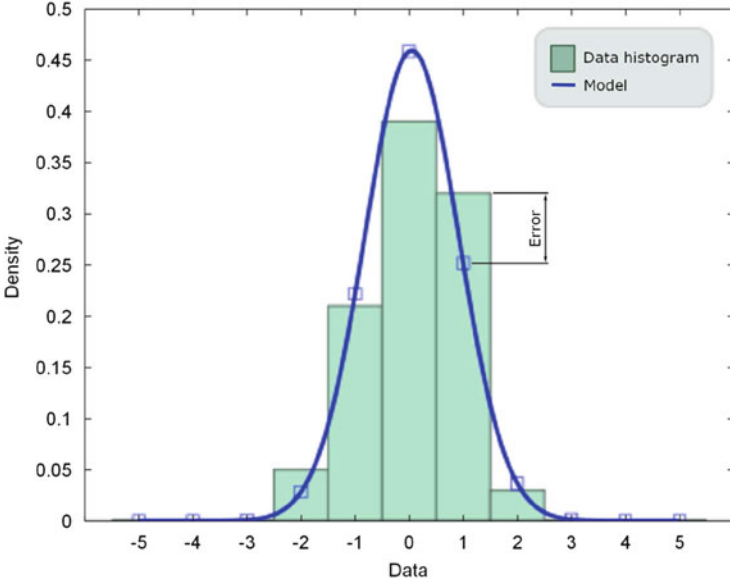


Fig. 7 Example error calculation between fitted distribution (model) and reference histogram [44]

Criteria for our systematic goodness of fit include:

- The comparison of any model against a reference histogram, with a given number of bins, is a metric. This metric is defined as the sum of errors (squared) between the model pdf and the reference histogram, evaluated at the histogram bin centres. The application of the metric is illustrated in Fig. 7, with histogram and fitted model.
- The number of parameters is given by the number of model options M over all sets, as well as the number of free-parameters, p_m , per option, $m = \{1, \dots, M\}$.

This is formulated as follows. Consider M ‘empirical models’ comprising univariate empirical histograms. Each histogram, $H_m, m = \{1 \dots, M\}$, comprises a set of values $H_m(\beta_b)$. Consider M ‘continuous models’, with density functions $F_m(\mathbf{x})$, that may be evaluated at histogram points β_b . An absolute goodness-of-fit \mathcal{G} follows as

$$\mathcal{G} \triangleq \underbrace{\frac{1}{MB} \sum_{m,b} |H_m(\beta_b) - F_m(\beta_b)|^2}_{\mathcal{E}} + \underbrace{\log_2 \left(\sum_{m=1}^M p_m \right)}_{\mathcal{C}}, \quad (6)$$

and the base-2 logarithm, $\log_2(\cdot)$ above, follows complexity suggestions of [21]. Note that in (6) we assume (very) large n , which implies that the complexity is predominantly due to the number of parameters similar to the AIC approach in (5), and hence we ignore the number of samples n .

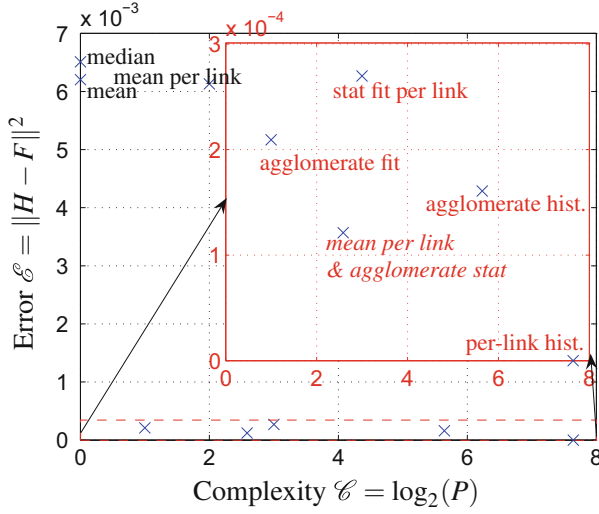


Fig. 8 Error versus complexity, first-order statistics, for the everyday data [41]. Note *insets* are the zoomed-in lower portions of graph

8.1.1 Evaluation of First-Order Statistics by Absolute Measure

With a subset of the complete open-access dataset in [43], the everyday activities of an adult male subject (height 1.84 m) over a period of 9 h are captured. There are $M = 4$ links (left/right-hip \rightarrow right wrist; left/right hip \rightarrow right-ankle) and the data contains over 2.9 million samples per link, sampled at 200 Hz. Figure 8 shows error \mathcal{E} vs complexity \mathcal{C} for various model options for the everyday data. Equivalent goodness \mathcal{G} is given by $\mathcal{E} + \mathcal{C} = \text{constant}$ and ‘better’ models will appear closer to the origin.

In all cases the lognormal distribution was the best-fit. The number of parameters for the *mean per-link & agglomerate stat* is $P = M + 2$, since there are M means, and 2 free parameters. In terms of goodness \mathcal{G} and as a trade-off between error \mathcal{E} and complexity \mathcal{C} , Fig. 8 shows that one of either: (a) a mean-per-link with a lognormal statistic (1) fitted to agglomerate data with mean-removed from each link (parameters $\mu_l = -1.02, \sigma_l = 0.87$); or (b) a lognormal fit to agglomerate data (parameters $\mu_l = -7.66, \sigma_l = 1.02$); is the preferable model. Option (a) is preferable in terms of \mathcal{E} , and (b) is preferable in terms of \mathcal{C} .

8.1.2 Evaluation of Second-Order Statistics by Absolute Measure

It is important to note that in various earlier radio propagation literature, direct statistical characterization of second-order statistics of level crossing intervals⁸ and

⁸Level-crossing interval is the inverse of level crossing rate.

fade durations has been performed, in, e.g., [27, 30]. Such an approach has been adopted in some BAN propagation characterization, in, e.g., [38, 46]. With direct characterization of second-order statistics we apply the same measure of (6) to ~ 150 h of the “everyday” on-body link dataset in [43]. We show some results for comparing different direct statistical characterization techniques for fade durations and level crossing intervals in Fig. 9.

Figure 9a, b show that the empirical histogram for all data sets gives zero error but excessive complexity, $P = MT$. Similarly, a combined histogram is also complex, $P = T$, and has moderate error. The error caused by using simple agglomerate mean level crossing interval, in Fig. 9a or simple agglomerate average fade duration at median channel gain in Fig. 9b, is very large. Similarly a set of mean level crossing intervals or average fade durations per link also has large error. For Fig. 9a

Fig. 9 Error v. complexity, second-order statistics [34]; LN-lognormal. (a) Error \mathcal{E} v. complexity \mathcal{C} for models of level crossing intervals with respect to median channel gains. Mean intervals range specified. (b) Error \mathcal{E} v. complexity \mathcal{C} for models of fade duration data with respect to median channel gains. Mean durations range specified

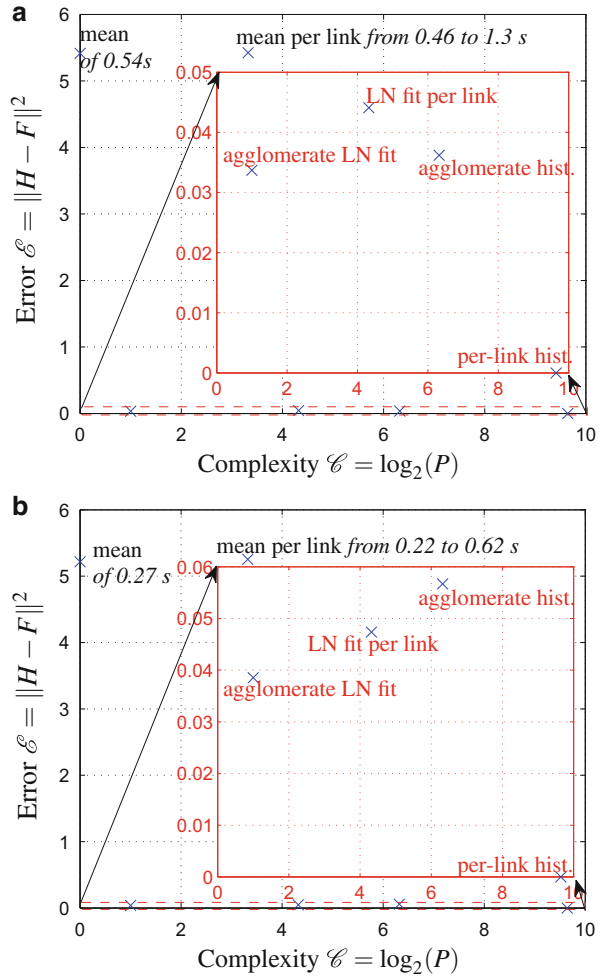


Table 5 Best lognormal (LN) agglomerate fits, parameters: μ_l is log-mean, σ_l is log-standard deviation

Statistic	LN parameters at h_{md}	LN parameters at h_m
Level crossing interval (s)	$\mu_l = -2.71, \sigma_l = 1.62$	$\mu_l = -2.78, \sigma_l = 1.68$
Fade duration (s)	$\mu_l = -3.81, \sigma_l = 1.65$	$\mu_l = -3.82, \sigma_l = 1.82$
Non-fade duration (s)	$\mu_l = -3.81, \sigma_l = 1.67$	$\mu_l = -3.93, \sigma_l = 1.56$

Statistics, in seconds (s), captured at median and mean channel gains, h_{md} and h_m respectively [34]

for level crossing intervals, and Fig. 9b for fade durations, goodness \mathcal{G} is clearly optimized across all links simply with a 2 parameter lognormal fit.

The best lognormal agglomerate fits, with respect to both mean and median channel gains (where channel gain is the inverse of path loss), for level crossing intervals, fade duration and non-fade duration data, measured in seconds, are summarized in Table 5. It can be observed that for respective statistics, whether fade duration, non-fade duration or level crossing interval, that the best lognormal fit is very similar (according to both parameters of log-mean and log-standard deviation) whether with respect to mean or median channel gains—even though mean channel gain is typically several-dB larger than the median gain.

9 Particularly Difficult Scenarios for BAN Operation

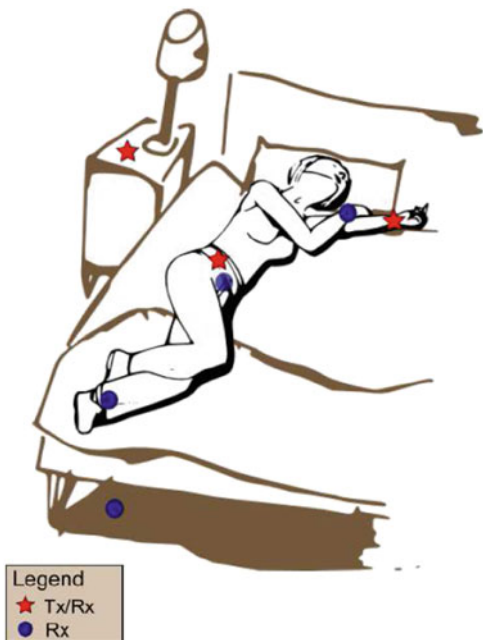
Although BANs may be used in any scenario, they are motivated from a healthcare viewpoint. As such, significant work is needed to ensure that the BAN is functional when a subject sleeps, and when a subject is in close proximity to others. Both scenarios are unusual and difficult from a wireless communication standpoint.

9.1 BAN Channels for Sleep-Monitoring

We demonstrate effective performance measures and show that transmit-receive (Tx-Rx) links are often in outages for periods of minutes over a range of receive sensitivities [42]. The outages are in excess of latency requirements for many medical BAN applications [25, 47], with a packet error rate greater than 10% at a very optimistic Rx sensitivity of -100 dBm, 100 dB below transmit power. The sleeping experiment set-up with the particular links is outlined in Fig. 10.

The on-body channel gain profiles for the left-wrist to the hip (back), and the off-body time series for the hip (front) to the radio next to the bed (head) are given in Fig. 11a, *There is clearly channel temporal stability with long periods of little movement while subjects are sleeping. The channel provides unreliable communications due to very low channel gain.* The empirical outage probability

Fig. 10 Illustration of the sleeping experiment set-up [42]



for the on-body and off-body channel is shown in Fig. 11b. The best case outage probability is more than 10 % for both on-body (13.5 %) and off-body (10.9 %) channels. Figure 11b illustrates that the packet error rate (PER) for a BAN radio will be at least 10 % for a standard one-hop star topology with a person sleeping—which demonstrates the need for relays, and potential two-hop links.

The sleeping channel is also best characterized with gamma fading. For the on-body sleeping channel the shape parameter $a = 1.60$, and the scale parameter $b = 0.480$; and for the off-body channel $a = 3.54$ and $b = 0.254$ [42], with median path losses of 80 dB for both these channels.

In [42] it is also shown that, e.g., a receiver with a sensitivity of -88 dBm, or 88 dB below transmit power of 0 dBm, will experience outages of larger than 1,000 s 5 % of the time. Further, in terms of BAN latency requirements for medical applications at 88 dB below transmit power for example, outages of larger than a typical latency requirement of 125 ms [25, 47], occur more than 22 % of the time.

9.2 Large Numbers of Co-located BANs

Up to 10 BANs must be capable of coexisting (operating properly) within a $6 \times 6 \times 6$ m³ cube. For example, if a group of subjects enters an elevator. BANs do not have a global coordination mechanism, hence understanding, and mitigating the interference of multiple co-located BANs, the body-to-body channel, becomes very important. Further it provides a particularly challenging scenario for the operation

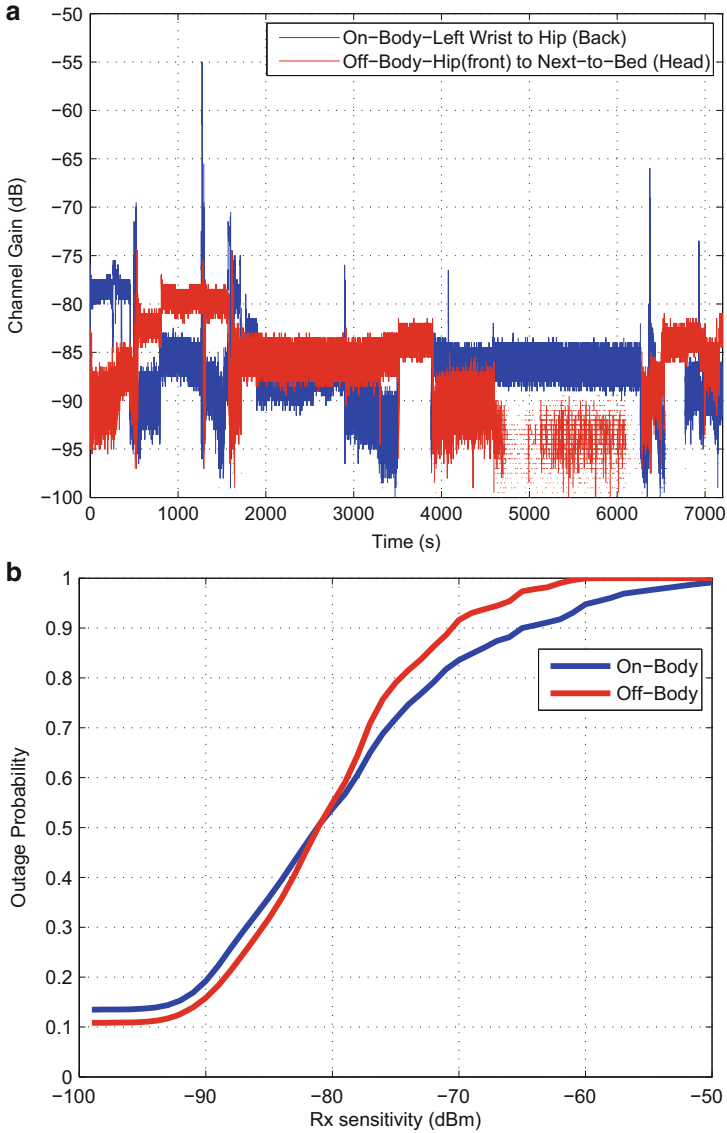


Fig. 11 Characterization of the impact that a subject sleeping has on channel outage [42]. (a) Typical on-body and off-body channel gain time series profile for the BAN sleep-monitoring channel. (b) Outage probability as a function of receive sensitivity, with Tx power of 0 dBm

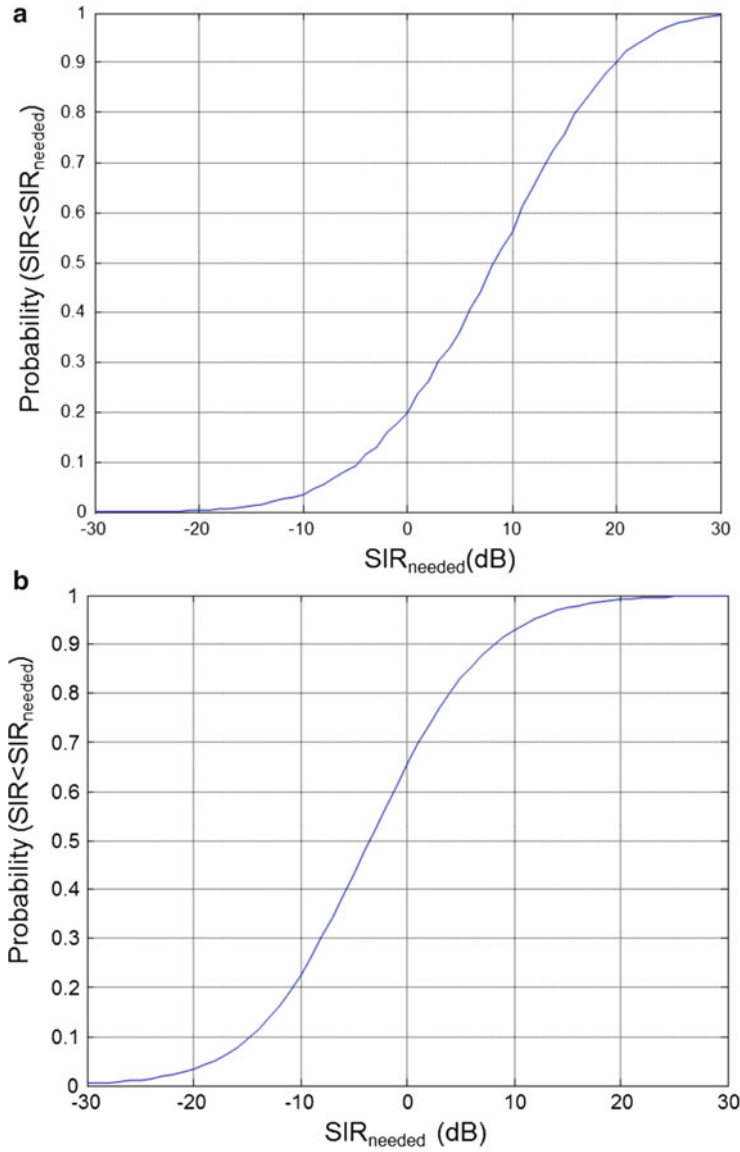


Fig. 12 CDF for required (needed) SIR to achieve outage probability value given in y-axis for co-located BANs [18]. (a) SIR outage for BAN with 1 co-channel interferer. (b) SIR outage for BAN with 9 co-channel interferers

of multiple BANs. To illustrate this in Fig. 12, we show from extensive interference measurements, that to ensure 10 % outage with 9 cochannel interferers, e.g., Tx/Rx links from 10 BANs operating in the same time-division-multiple-access (TDMA) time slot, the SIR that needs to be tolerated is -15 dB, Fig. 12b, with one co-channel interferer this is -5 dB, Fig. 12a, [18]. This is very difficult, and underlines the need for interference mitigation techniques including significant duty cycling to ensure best operation, and demonstrates that re-transmits may often be necessary when significant numbers of BANs are co-located.

10 Conclusion

In this chapter we have investigated channel modeling for wireless body area networks (BANs). We have shown that the BAN radio channel is particularly different from other typical radio channels—and in consideration of the stated technical requirements for BANs as they employ ultra-low-power short-range radios, there are many challenges presented to the radio system designer, including large path losses and non wide-sense-stationarity over any significant length of time. But, as described, there are mitigating benefits, including BAN channel temporal stability and channel reciprocity. We have highlighted the importance of mitigating interference with large numbers of co-located, non globally-coordinated, BANs, as well as other difficult channels for BAN operation, such as sleep monitoring. Also emphasized has been the importance of long-term radio channel measurements, to use as the basis for radio design, particularly considering non wide-sense-stationarity. In terms of first-order statistics, lognormal, and sometimes gamma or Weibull distributed fading characterizations have been shown to be most prevalent, but Rayleigh fading *is not a good characterization*. Finally an alternative means of evaluation, using an absolute histogram representation with respect to measurements, has been described that is very helpful in deciding the best characterization of the BAN channel, for both first and second-order statistics.

References

1. A. Abdi, M. Kaveh, On the utility of gamma pdf in modeling shadow fading (slow fading), in *IEEE 49th Vehicular Technology Conference*, vol. 3 (1999), pp. 2308–2312 doi:10.1109/VETEC.1999.778479
2. H. Akaike, A new look at the statistical model identification. *IEEE Trans. Autom. Control* **19**(6), 716–723 (1974)
3. A. Alomainy, Y. Hao, Radio channel models for UWB body-centric networks with compact planar antenna, in *IEEE Antennas and Propagation Society International Symposium* (IEEE, Albuquerque, NM, 2006), pp. 2173–2176
4. A. Alomainy, Y. Hao, Modeling and characterization of biotelemetric radio channel from ingested implants considering organ contents. *IEEE Trans. Antennas Propag.* **57**(4), 999–1005 (2009). doi:10.1109/TAP.2009.2014531

5. A. Alomainy, Y. Hao, Y. Yuan, Y. Liu, Modelling and characterisation of radio propagation from wireless implants at different frequencies, in *The 9th European Conference on Wireless Technology*, Manchester, 2006, pp. 119–122. doi:10.1109/ECWT.2006.280449
6. V. Chaganti, L. Hanlen, D. Smith, Are narrowband wireless on-body networks wide-sense stationary? *IEEE Trans. Wirel. Commun.* **13**(5), 2432–2442 (2014). doi:10.1109/TWC.2014.031914.130303
7. X. Chen, X. Lu, D. Jin, L. Su, L. Zeng, Channel modeling of UWB-based wireless body area networks, in *IEEE International Conference on Communications (ICC)*, Kyoto, 2011, pp. 1–5. doi:10.1109/icc.2011.5962687
8. S.L. Cotton, W.G. Scanlon, A statistical analysis of indoor multipath fading for a narrowband wireless body area network, in *IEEE Personal, Indoor and Mobile Radio Communications Symposium, PIMRC 2006*, Helsinki, 2006, pp. 1–5
9. S.L. Cotton, W.G. Scanlon, Higher-order statistics for the κ - μ distribution. *Electron. Lett.* **43**(22), 1215–1217 (2007)
10. S.L. Cotton, R. D’Errico, C. Oestges, A review of radio channel models for body centric communications. *Radio Sci.* **49**(6), 371–388 (2014)
11. R. D’Errico, L. Ouvry, Delay dispersion of the on-body dynamic channel, in *Proceedings of the Fourth European Conference on Antennas and Propagation (EuCAP)*, Barcelona, 2010, pp. 1–5
12. R. D’Errico, L. Ouvry, A statistical model for on-body dynamic channels. *Int. J. Wirel. Inf. Netw.* **17**, 92–104 (2010)
13. Federal Communications Commission (FCC) Guidelines. (1997) [Online] <http://www.fcc.gov/oet/rfsafety/sar.html#sec1>
14. A. Fort, Body area communications: channel characterization and ultra-wideband system-level approach for low power, Ph.D thesis, Vrije Universiteit Brussel, Brussels, 2007
15. A. Fort, C. Desset, P. De Doncker, P. Wambacq, L. Van Biesen, An ultra-wideband body area propagation channel model—from statistics to implementation. *IEEE Trans. Microw. Theory Tech.* **54**(4), 1820–1826 (2006)
16. A. Fort, J. Ryckaert, C. Desset, P. De Doncker, P. Wambacq, L. Van Biesen, Ultra-wideband channel model for communication around the human body. *IEEE J. Sel. Areas Commun.* **24**(4), 927–933 (2006)
17. A. Fort, C. Desset, P. Wambacq, L. Biesen, Indoor body-area channel model for narrowband communications. *IET Microw. Antennas Propag.* **1**(6), 1197–1203 (2007)
18. L. Hanlen, D. Miniutti, D. Smith, A. Zhang, D. Rodda, B. Gilbert, A. Boulis, Network-to-network interference measurements ID: 802.15-09-0520-01-0006. IEEE Submission (2009)
19. L.W. Hanlen, V.G. Chaganti, B. Gilbert, D. Rodda, T. Lamahewa, D.B. Smith, Open-source testbed for body area networks: 200 sample/sec, 12 hrs continuous measurement, in *IEEE International Symposium on Personal, Indoor and Mobile Radio Communications (PIMRC)*, Istanbul, 2010, pp. 66–71
20. L.W. Hanlen, D. Miniutti, D.B. Smith, D. Rodda, B. Gilbert, Co-Channel interference in body area networks with indoor measurements at 2.4 GHz: distance-to-interferer is a poor estimate of received interference power. *Int. J. Wirel. Inf. Netw.* **17**, 113–125 (2010)
21. R.V.L. Hartley, Transmission of information. *Bell Syst. Tech. J.* **7**(3), 535–563 (1928)
22. Z.H. Hu, Y. Nechayev, P. Hall, Measurements and statistical analysis of the transmission channel between two wireless body area networks at 2.45 GHz and 5.8 GHz, in *ICECom, 2010 Conference Proceedings* (IEEE, 2010), pp. 1–4
23. IEEE standard for local and metropolitan area networks part 15.6: wireless body area networks. *IEEE Std 802156-2012* (2012), pp. 1–271. doi:10.1109/IEEESTD.2012.6161600
24. M. Kim, J.I. Takada, Statistical model for 4.5-GHz narrowband on-body propagation channel with specific actions. *IEEE Antennas Wirel. Propag. Lett.* **8**, 1250–1254 (2009). doi:10.1109/LAWP.2009.2036570
25. D. Lewis, 802.15.6 call for applications - response summary ID: 802.15-08-0407-05. IEEE Submission (2008)

26. H. Luecken, T. Zasowski, C. Steiner, F. Troesch, A. Wittneben, Location-aware adaptation and precoding for low complexity IR-UWB receivers, in *IEEE International Conference on Ultra-Wideband, 2008. ICUWB 2008*, vol. 3, Hannover, 2008, pp. 31–34. doi:10.1109/ICUWB.2008.4653409
27. T. Mimaki, H. Sato, M. Tanabe, A study on the multi-peak properties of the level-crossing intervals of a random process. *Signal Process.* **7**(3), 251–265 (1984)
28. D. Miniutti, L.W. Hanlen, D.B. Smith, J.A. Zhang, D. Lewis, D. Rodda, B. Gilbert, Narrowband channel characterization for body area networks ID: 802.15.08.0421. IEEE Submission (2008)
29. A.F. Molisch, D. Cassioli, C.C. Chong, S. Emami, A. Fort, B. Kannan, J. Karedal, J. Kunisch, A comprehensive standardized model for ultrawideband propagation channels. *IEEE Trans. Antennas Propag.* **54**(11), 3151–3166 (2006)
30. S. Rice, Distribution of the duration of fades in radio transmission: Gaussian noise model. *Bell Syst. Tech. J.* **37**(3), 581–635 (1958)
31. C. Roblin, J.M. Laheurte, R. D'Errico, A. Gati, D. Lautru, T. Alvès, H. Terchoune, F. Bouttout, Antenna design and channel modeling in the BAN context part i: antennas. *Ann. Telecommun.* **66**, 139–155 (2011)
32. K. Sayrafian-Pour, W.B. Yang, J. Hagedorn, J. Terrill, K.Y. Yazdandoost, K. Hamaguchi, Channel models for medical implant communication. *Int. J. Wirel. Inf. Netw.* **17**(3–4), 105–112 (2010)
33. T.S. See, J. Hee, C. Ong, L. Ong, Z.N. Chen, Inter-body channel model for UWB communications, in *Proceedings of the Third European Conference on Antennas and Propagation (EuCAP) 2009*, Berlin, 2009, pp. 3519–3522
34. D.B. Smith, L.W. Hanlen, The body area network channel model: a new look at second-order statistics, in *Proceedings of the Eighth European Conference on Antennas and Propagation (EuCAP)*, The Hague, 2014, pp. 4351–4354
35. D.B. Smith, L.W. Hanlen, D. Miniutti, J.A. Zhang, D. Rodda, B. Gilbert, Statistical characterization of the dynamic narrowband body area channel, in *International symposium on applied sciences in biomedical and communication (ISABEL)*, Aalborg, 2008, pp. 1–5
36. D. Smith, D. Miniutti, L. Hanlen, A. Zhang, D. Lewis, D. Rodda, B. Gilbert, Power delay profiles for dynamic narrowband body area network channels id:15-09-0187-01-0006. IEEE Submission (2009)
37. D. Smith, J. Zhang, L. Hanlen, D. Miniutti, D. Rodda, B. Gilbert, Temporal correlation of dynamic on-body area radio channel. *Electron. Lett.* **45**(24), 1212–1213 (2009). doi:10.1049/el.2009.2057
38. D. Smith, D. Miniutti, L.W. Hanlen, D. Rodda, B. Gilbert, Dynamic narrowband body area communications: link-margin based performance analysis and second-order temporal statistics, in *IEEE Wireless Communications and Networking Conference (WCNC)*, Sydney, 2010, pp. 1–6
39. D. Smith, L. Hanlen, J. Zhang, D. Miniutti, D. Rodda, B. Gilbert, First- and second-order statistical characterizations of the dynamic body area propagation channel of various bandwidths. *Ann. Telecommun.* **66**, 187–203 (2011)
40. D. Smith, T. Lamahewa, L. Hanlen, F. Miniutti, Simple prediction-based power control for the on-body area communications channel, in *IEEE International Conference on Communications (ICC)* (2011), pp. 1–5. doi:10.1109/icc.2011.5963355
41. D.B. Smith, L.W. Hanlen, T.A. Lamahewa, A new look at the body area network channel model, in *Proceedings of the Fifth European Conference on Antennas and Propagation (EuCAP)*, Rome, 2011, pp. 2987–2991
42. D.B. Smith, D. Miniutti, L.W. Hanlen, Characterization of the body-area propagation channel for monitoring a subject sleeping. *IEEE Trans. Antennas Propag.* **59**(11), 4388–4392 (2011). doi:10.1109/TAP.2011.2164209
43. D. Smith, L. Hanlen, D. Rodda, B. Gilbert, J. Dong, V. Chaganti, Body Area Network Radio Channel Measurement Set (2012). [Online] <http://opennicta.com/datasets>

44. D. Smith, D. Miniutti, T. Lamahewa, L. Hanlen, Propagation models for body-area networks: a survey and new outlook. *IEEE Antennas Propag. Mag.* **55**(5), 97–117 (2013). doi:10.1109/MAP.2013.6735479
45. X.D. Yang, Q. Abbasi, A. Alomainy, Y. Hao, Spatial correlation analysis of on-body radio channels considering statistical significance. *IEEE Antennas Wirel. Propag. Lett.* **10**, 780–783 (2011). doi:10.1109/LAWP.2011.2163378
46. K. Yazdandoost, K. Sayrafian-Pour, TG6 channel model ID: 802.15-08-0780-12-0006. *IEEE Submission* (2010)
47. B. Zhen, M. Patel, S. Lee, E. Won, Body area network (BAN) technical requirements ID:15-08-0037-01-0006. *IEEE Submission* (2008)
48. B. Zhen, K. Takizawa, T. Aoyagi, R. Kohno, A body surface coordinator for implanted biosensor networks, in *IEEE International Conference on Communications, ICC '09*, Dresden, 2009, pp. 1–5. doi:10.1109/ICC.2009.5198579

Ultra-Low-Power Short-Range Radios

Mercier, P.P.; Chandrakasan, A.P. (Eds.)

2015, XII, 394 p. 307 illus., 139 illus. in color.,

Hardcover

ISBN: 978-3-319-14713-0